

## Study of the Growth of Thin Epitaxial CVD Diamond Films on Silicon

S. Geier<sup>1</sup>, R. Hessmer<sup>1</sup>, M. Schreck<sup>1</sup>, B. Stritzker<sup>1</sup>, B. Rauschenbach<sup>1</sup>,  
K. Helming<sup>2</sup>, K. Kunze<sup>3</sup> and W. Erfurth<sup>4</sup>

<sup>1</sup> Institut für Physik, Universität Augsburg, D-86135 Augsburg, Germany

<sup>2</sup> Institut für Metallkunde und Metallphysik, TU Clausthal, D-38678 Clausthal-Zellerfeld, Germany

<sup>3</sup> Geologisches Institut, ETH-Zentrum, CH-8092 Zürich, Switzerland

<sup>4</sup> Max-Planck-Institut für Mikrostrukturphysik, D-06120 Halle/S., Germany

**Keywords:** CVD Diamond, Thin Film, Growth, Texture, Epitaxy

### ABSTRACT

The growth characteristic of thin diamond films grown on Si(001) substrates by microwave plasma enhanced chemical vapor deposition (CVD) has been investigated. Using synchrotron radiation X-ray diffractometry (XRD) has been employed for pole figure measurements in order to study the global texture of the films during the initial growth stage. The analysis by the component method allowed to reproduce the texture quantitatively elucidating the heteroepitaxial orientational relationship and the strong occurrence of twinning. Also, the fraction of randomly oriented crystallites in the film has been determined. With increasing film thickness the process of evolutionary growth results in the overgrowth of twins and in the narrowing of the pole density maxima of the epitaxial component. A detailed study of the full width at half maximum (FWHM) of these pole density maxima as a function of the film thickness allows to draw first conclusions on the distribution of the epitaxial crystallites around their preferred orientation. Furthermore, orientation imaging microscopy (OIM) has been employed to study the crystallite defect structure at the interface.

### 1. INTRODUCTION

The single crystal properties of natural diamond have led to the prediction of considerable advances in electronics to be made using diamond as an electronic material [1]. It especially qualifies for high temperature, high power and high frequency electronics devices [2]. To utilize diamond as a semiconductor material from which to fabricate electronic devices, it is necessary to produce single-crystal thin films over large areas. Because of economical and technological reasons the heteroepitaxial growth of diamond films on silicon substrates is an important goal. Despite the large lattice mismatch of 52% between diamond and silicon heteroepitaxy has been reported by chemical vapor deposition [3]. Besides the orientational spread of the epitaxial crystallites around the orientation of the silicon substrate their corresponding twins have been observed [4, 5].

The purpose of the present work is the quantitative determination of the texture of diamond films during the initial growth stage, the study of the influence of film growth on the orientational distribution of the crystallites, and a visualization of the crystallite defect structure.

## 2. EXPERIMENTAL

Diamond films have been grown on Si(001)-substrates by microwave plasma CVD using a commercial deposition system. The thickness of the deposited layers ranges from 100 nm up to 37  $\mu\text{m}$ . The substrates have been etched in situ in a hydrogen plasma to remove the oxide layer. Subsequently, the film deposition has been carried out in a two step process. First, for the nucleation of oriented grains a biasing step has been employed where the substrate was set at -200V with respect to the plasma. Second, normal growth on the predeposited surface has been realized after turning off the voltage. For details on the process parameters and preparation conditions, see Refs. 5 and 6.

The surface morphology of the deposited diamond layers has been analyzed by scanning electron microscopy.

The pole figure measurement on the 100 nm thick diamond layer has been performed at the German synchrotron radiation source DESY ( $\lambda=0.154$  nm, Si double crystal monochromator in the primary beam). For the thicker samples (thickness $\geq 600$  nm) a commercial Cu X-ray tube has been used in combination with a curved graphite monochromator in front of the detector. In both cases an Eulerian cradle allowed to rotate the diamond film around an axis normal (azimuth angle  $\varphi$ ) and parallel (polar angle  $\chi$ ) to the substrate. The angular step sizes have been  $\Delta\varphi=\Delta\chi=2^\circ$ . For the determination of the values of the broadening of the pole density maxima corresponding to the epitaxially aligned crystallites  $\chi$ - and  $\varphi$ -scans have been employed with a smaller step size in order to increase the resolution, which was then less than  $1^\circ$  in  $\chi$  and  $\varphi$ . The presented values of full width at half maximum for the pole density maxima along the polar and azimuthal direction ( $\text{FWHM}_{\text{tilt}}$  and  $\text{FWHM}_{\text{rot}}$ ) have been obtained by  $\chi$ -scans in {111}-reflection geometry and by  $\varphi$ -scans in {220}-transmission geometry, respectively. Thus, the results of  $\text{FWHM}_{\text{tilt}}$  and  $\text{FWHM}_{\text{rot}}$  are a direct measure for the polar and azimuthal misalignment of the epitaxial crystallites (tilt against and rotation around the substrate normal), respectively.

Orientation imaging microscopy (OIM) [7] has been used for visualizing the crystallite defect structure directly at the interface. For that purpose the silicon substrate has been removed prior to the measurement after stabilizing the film by silver epoxy. OIM is based on the coupling of the automated analysis of electron backscattering Kikuchi diffraction patterns with the precise positioning of the sample in the scanning electron microscope. The interaction of the incident electron beam with the sample produces backscattered electrons which are detected on a fluorescent screen mounted in the vacuum chamber. This diffraction image is transmitted to the computer and the analysis yields the orientation of the crystal lattice at the beam location in terms of the complete set of Eulerian angles. The lateral resolution is about 0.25  $\mu\text{m}$ . The information depth for diamond is about 40 nm [8].

## 3. TEXTURE ANALYSIS BY THE COMPONENT METHOD

The component method [9, 10] allows to approximate the orientation density function (ODF) as a sum of components by identifying preferred directions in the measured pole figures. From the ODF pole figures for any crystal direction can be recalculated. Furthermore, the randomly oriented fraction of crystallites is quantifiable.

A texture component  $c$  is described by its preferred orientation  $g^c=(\alpha^c, \beta^c, \gamma^c)$ , a certain spread of orientation  $b^c$  (FWHM of a Gauss function) and the component intensity  $I^c$ , which corresponds to the volume fraction of all crystallites that belong to the component.

#### 4. RESULTS

Figure 1a displays a scanning electron micrograph of a 100 nm thick diamond film on Si(001). The surface morphology indicates qualitatively an island-growth characteristic. Figure 1b shows a 90°-section of the {111}-pole figure of this film.

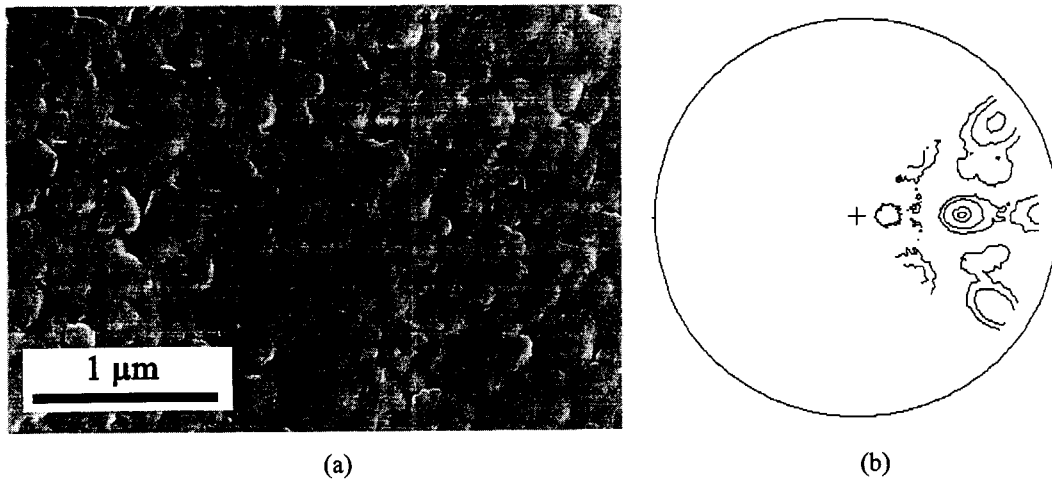


FIG.1 SEM-micrograph of a 100 nm thick diamond film on a Si(001)-substrate (a) and a 90°-section of the corresponding {111}-pole figure (b). Contour levels in (b): 0.9, 1.5, 2.0, 3.0;

The texture analysis by the component method resulted in an approximation of the ODF by summarizing over 13 components (see Table 1). By these components 25% of the total volume of the crystallites in the film could be comprised, i.e. 75% of the grains are randomly oriented. The first component ( $I^1=19.2\%$ ) can be attributed to epitaxially aligned crystallites, whose preferred orientation is identical to the substrate orientation. The components 2-5 ( $I^{2-5} = 31.6\%$ ) and 6-13 ( $I^{6-13} = 49.2\%$ ) correspond to their twins of first and second order, respectively. From the high intensity values for the latter components we draw the conclusion, that the process of twinning plays the dominant role during the initial growth stage.

TABLE 1.

Table of texture components of a 100 nm thick diamond film on Si(001). Each component is characterized by the intensity portion  $I^c$  (regarding the textured fraction of crystallites in the film), the FWHM  $b^c$  and the orientation  $g^c = \{\alpha^c, \beta^c, \gamma^c\}$ .

comp. c	1	2	3	4	5	6	7	8	9	10	11	12	13
$I^c$ [%]	19.2	7.9	7.9	7.9	7.9	8.3	8.3	4.0	4.0	8.3	8.3	4.0	4.0
$b^c$ [°]	8.8	8.5	8.6	8.5	8.6	12.2	11.9	10.6	10.3	12.2	11.9	10.6	10.3
$\alpha^c$ [°]	269	341	251	161	71	299	210	63	333	119	30	243	153
$\beta^c$ [°]	2	48	48	48	48	25	25	24	24	25	25	24	24
$\gamma^c$ [°]	45	26	26	26	26	77	76	9	10	77	76	9	10

Based on the approximated ODF the {111}-pole figure has been recalculated. The result is seen in Fig. 2b. The uncomplete measured pole figure of Fig. 1a has been completed in  $\phi$  according to the symmetry of the Si(001)/diamond film system (Fig.2a). Comparing the theoretically to the experimentally determined pole figure it is noticed that deviations in the pole density are only restricted to weak intensity maxima. The relative error of deviation is about 30% [10]. Four

components of twins of second order could not be considered for the ODF approximation because of asymmetries in the pole figure of Fig. 1a which are due to uncertainties of thin film measurements and the inhomogeneity of the sample. As a consequence, the determined fraction of 19.2% for epitaxial crystallites can be considered as an upper limit.

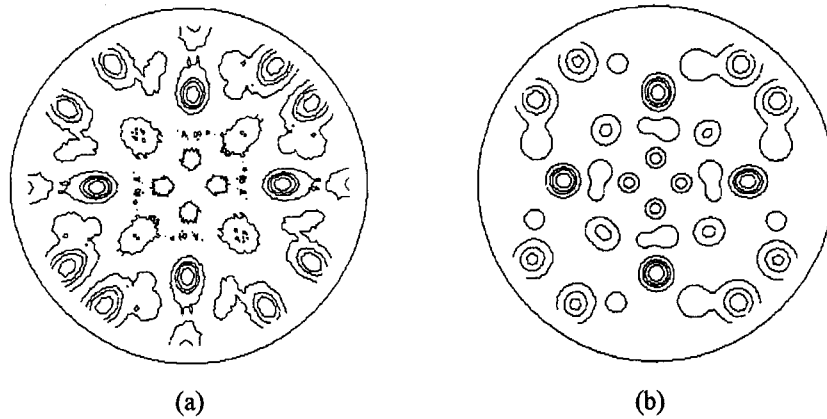


FIG. 2. {111}-pole figure of a 100 nm thick diamond film on Si(001) experimentally determined by XRD (a) and recalculated by the component method (b). Contour levels: 0.9, 1.5, 2.0, 3.0;

In the following diamond films with thicknesses up to 37  $\mu\text{m}$  have been investigated. For a 600 nm thick layer the film morphology shows first faceting (Fig. 3a) and in comparison to the initial growth stage epitaxially aligned crystallites dominate, whereas their twins of first and second order are placed at a disadvantage during the textured growth process (Fig. 3b).

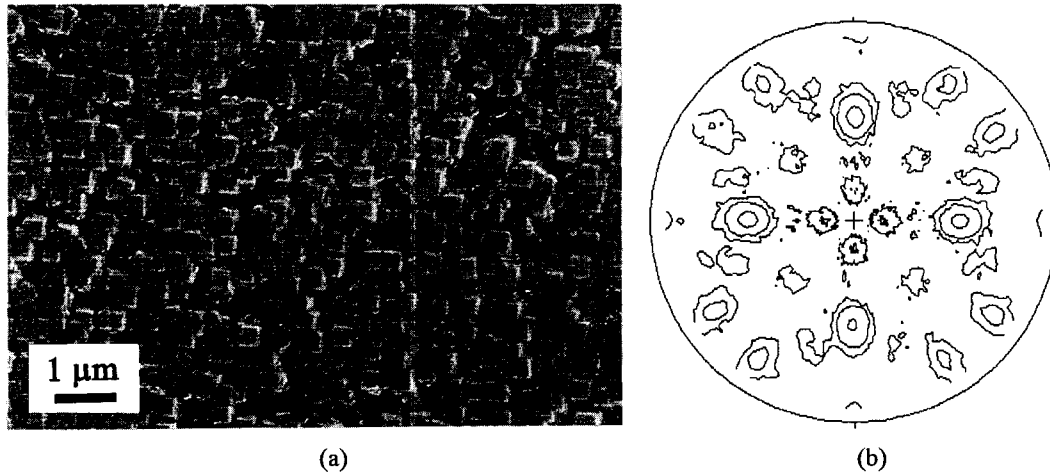


FIG. 3. SEM-micrograph of a 600 nm thick diamond film on a Si(001)-substrate (a) and the corresponding {111}-pole figure (b). Contour levels in (b): 0.75, 2.5, 20.0;

At the surface of a 9  $\mu\text{m}$  thick diamond film the crystallites show clear {001}-facets and are well aligned to each other (Fig. 4a). The volume fraction of twinned crystallites in the film is negligible (Fig. 4b).

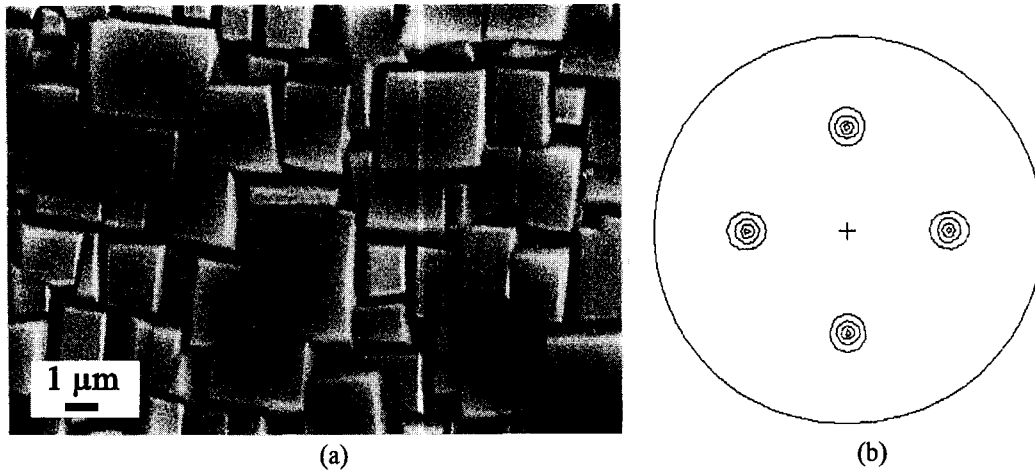


FIG.4. SEM-micrograph of a 9  $\mu\text{m}$  thick diamond film on a Si(001)-substrate (a) and the corresponding  $\{111\}$ -pole figure (b). Contour levels in (b): 1, 10, 50, 100;

In the following the improvement of the film texture is studied by focusing on the narrowing of the pole density maxima of the epitaxial component with increasing film thickness. Figure 4 shows the experimentally determined values of  $\text{FWHM}_{\text{tilt}}$  and  $\text{FWHM}_{\text{rot}}$ . Due to the textured growth process  $\text{FWHM}_{\text{tilt}}$  decreases with increasing film thickness (thickness range: 100 nm to 37  $\mu\text{m}$ ), whereas  $\text{FWHM}_{\text{rot}}$  is roughly constant [6].

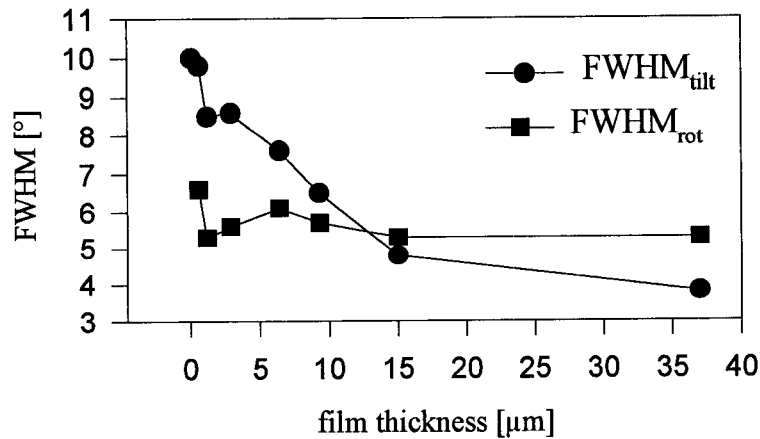


FIG.5.  $\text{FWHM}_{\text{tilt}}$  and  $\text{FWHM}_{\text{rot}}$  as a function of film thickness. The values are a direct measure for the misalignment of the epitaxial crystallites in terms of tilt against and rotation around the substrate normal, respectively.

In order to study the crystallite defect structure OIM has been employed at the interface. The nucleation density of the investigated diamond layer has been chosen to be very low ( $10^6 \text{ cm}^{-2}$ ) in order to get crystallite sizes of the order of 10  $\mu\text{m}$ . Figure 5 displays a grain boundary map of two diamond crystallites over an area of  $60 \times 30 \mu\text{m}^2$ . The thick boundary lines, which correspond to  $\Sigma=3$ -twin boundaries, start from the centers of the crystallites.

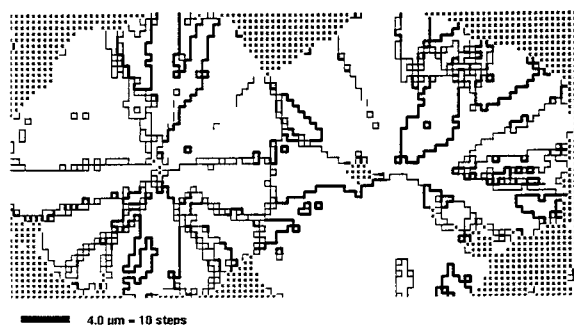


FIG.6.

Grain boundary map reconstructed from OIM measurements on two diamond crystallites at the diamond/silicon interface over an area of  $60 \times 30 \mu\text{m}^2$  using a step size of  $0.4 \mu\text{m}$ . Thin boundary line segments correspond to orientation distances greater than  $5^\circ$  between neighboring points. Thick boundary line segments are drawn if the orientation difference corresponds to  $\Sigma=3$ -twin boundaries.

## 5. CONCLUSIONS

The texture analysis on very thin films has shown that initial diamond islands contain an epitaxially aligned component (same orientation as the substrate) and their twins of first and second order. The quantification of the corresponding volume fractions indicates that twinning plays the dominant role during the initial growth stage. This is compatible with the image of the crystallite defect structure at the interface which shows mainly  $\Sigma=3$ -twin boundaries starting at the center of the crystallite. With increasing film thickness the texture can be improved by an appropriate growth step which results in an overgrowth of twins and in the narrowing of the pole density maxima of the epitaxial component. Crystallites with the axis of fastest growth parallel to the surface normal overgrow differently oriented grains. The rotational misalignment of the epitaxial crystallites ( $\text{FWHM}_{\text{rot}}$ ) is roughly constant as a function of increasing film thickness. This might be a first indication that the tilt against and the rotation around the substrate normal do not depend on each other. As a consequence, the occurrence of grain boundaries due to the rotational misalignment of the epitaxial crystallites cannot be reduced by depositing very thick films. On the other hand the rotational misalignment in terms of  $\text{FWHM}_{\text{rot}}$  is a parameter easy to determine for arbitrary film thicknesses in order to optimize the nucleation step.

## ACKNOWLEDGEMENTS

The authors gratefully acknowledge the assistance by Dr. S. Doyle and Dr. T. Wroblewski (DESY, Hamburg).

## REFERENCES

- [1] J. Wilks, *Properties and Applications of Diamond*, Butterworth-Heinemann, Oxford (1991)
- [2] M. Simpson, *New Sci.* **117**, 50 (1988)
- [3] X. Jiang and C.-P. Klages, *Diamond Relat. Mater.* **2**, 1112 (1993)
- [4] R. Kohl, C. Wild, N. Herres, P. Koidl, B. R. Stoner, and J. T. Glass, *Appl. Phys. Lett.* **63**, 1792 (1993)
- [5] M. Schreck, R. Hessmer, S. Geier, B. Rauschenbach, and B. Stritzker, *Diamond Relat. Mater.* **3**, 510 (1994)
- [6] R. Hessmer, M. Schreck, S. Geier, B. Rauschenbach, and B. Stritzker, *Diamond Relat. Mater.* **4**, 410 (1995)
- [7] B. L. Adams, S. I. Wright, and K. Kunze, *Metall. Trans. A* **24**, 819 (1993)
- [8] S. Geier, M. Schreck, R. Hessmer, B. Rauschenbach, B. Stritzker, K. Kunze, and B. L. Adams, *Appl. Phys. Lett.* **65**, 1781 (1994)
- [9] K. Helming and T. Eschner, *Cryst. Res. Technol.* **25**, K203 (1990)
- [10] K. Helming, S. Geier, M. Schreck, R. Hessmer, B. Stritzker, and B. Rauschenbach, *J. Appl. Phys.* **77**, 4765 (1995)